

Inverse gas chromatography of chromia. Part II. Finite surface coverage

A. E. ONJIA^{*#}, S. K. MILONJIĆ^{*#} and LJ. V. RAJAKOVIĆ^{**#}

^{*}*The Vinča Institute of Nuclear Sciences, P. O. Box 522, YU-11001 Belgrade and* ^{**}*Faculty of Technology and Metallurgy, P. O. Box 494, YU-11001 Belgrade, Yugoslavia*

(Received 5 July 2001)

The interactions of *n*-hexane, benzene, chloroform, and tetrahydrofuran with dried (amorphous) chromia (I) and chromia heated at 1073 K (crystalline) (II), both obtained from a colloidal dispersion, and a commercially available chromia (III) were studied by inverse gas chromatography (IGC) under finite surface coverage conditions. The isotherms, in the temperature range 383 – 423 K, were used to estimate the surface area, the adsorption energy distribution, the isosteric heat of adsorption, and the spreading pressure on the surfaces of the solids. The uniformly reduced adsorption ability of the heated chromia was attributed to the dehydroxylation of the surface at the higher temperatures. Both solids showed an increased affinity toward chloroform molecules, as a result of strong acid-base interaction.

Keywords: inverse gas chromatography, chromia, adsorption, organics, isotherms, isosteric heat.

INTRODUCTION

Adsorption onto the chromia surface occurs in many technological systems, such as catalysis, ceramics, microelectronics, painting, flotation, cosmetics, nutrition, and so on. Also, it takes part in processes occurring in the environment. In both the gas-solid and liquid-solid interface, the nature of the intermolecular interactions across the interfaces are of great importance, and often govern the overall process.¹

In the first part of this work,² inverse gas chromatography (IGC) at zero surface coverage was applied to investigate the surface characteristics (the dispersive components of the surface free energies, enthalpies, entropies, and the acid/base constants) of the solids obtained from colloidal chromia, by means of their interaction with different organics, and to examine the effects of the heat treatment on the adsorption characteristics. This paper presents data on the determination of the adsorption isotherms, the isosteric heat of adsorption, the adsorption energy distribution, and the spreading pressures, for the adsorption of several common organic molecules.

Serbian Chemical Society active member.

IGC has been applied for several decades as a method for obtaining the sorption isotherms of various organic compounds on a solid surface. The theory relating the chromatographic data to the adsorption parameters has been thoroughly reviewed elsewhere.^{3,4} Under finite coverage conditions, the retention volume depends on the amount of adsorbate in the gas phase, resulting in non-ideal isotherms and, hence, asymmetrical peak shapes. Using the ideal gas law, the amount of an organic compound adsorbed onto an adsorbent packed into a chromatography column, α , may be estimated from the common relation⁴:

$$\alpha = \frac{1}{mRT} \int_0^p V_N dp \quad (1)$$

The terms in the equations are given in the list of symbols. Provided that the adsorbate density, molecular weight, as well as the volume injected are accurately known, and F_c remains constant, the partial pressure of an adsorbate, p , may be calculated as follows⁴:

$$p = \frac{RTnh}{F_c S} \quad (2)$$

The flow rate of the mobile phase, usually measured at the column outlet, is converted to the corrected flow rate, F_c , for column temperature, T , using the James-Martin gas compressibility correction factor, j .⁵ This correction is important due to the sorption effect introduced when the mole fraction of adsorbate exceeds 0.01.⁴

The term $\alpha = f(p)$ in Eq. (1) is one form of the adsorption isotherm. In practice, $\alpha = f(p)$ is found using the expression⁶:

$$\alpha = \frac{S_{\text{ads}} n}{mS} \quad (3)$$

Hence, from the $\alpha(p)$ –(p) data, it is possible to draw the adsorption isotherm and to evaluate the related parameters.

EXPERIMENTAL

The adsorbent in solid form was prepared by controlled coagulation of a stable chromia dispersion, followed by extensive washing of the precipitate with deionized water. The material was then dried in an air oven at 150 °C for 24 h. A portion of the obtained solid was further treated by heating at 800 °C for (additional) 4 h. These two solids were denoted as (I) and (II), respectively. The third used sorbent (III) was a commercially available chromia (Fluka 27085).

The obtained materials were investigated by inductively coupled plasma atomic emission spectroscopy (ICP-AES), energy dispersive X-ray spectrometry (EDXRF) and X-ray diffraction (XRD). ICP-AES and EDXRF showed the presence of trace amounts of potassium, chlorine, aluminum and calcium. According to XRD, the obtained solid structure (I) was amorphous whereas solid (II) was demonstrated to have crystalline form.

All the solids were sieved through 0.1 mm mesh sieves and poured into a 0.25 m long (2.2 mm ID) stainless steel chromatographic column. After the column had been conditioned, overnight in a nitrogen flow at 150 °C, IGC experiments were performed. The BET specific surface area of the solids was measured using the nitrogen gas adsorption method after completion of the IGC experiments.

Retention data were obtained using a Spectra-physics model SP7100 gas chromatograph with a flame ionization detector (FID). Varian Star 4.5 software was applied to collect and compute the data. The FID was maintained at 250 °C, the injector at 220 °C, and the column temperature was in the range of 110 to 150 °C with 10 °C intervals. Purified nitrogen was used as the carrier gas at a flow rate of 3.0 ml/min. Methane was used as an unretained compound to determine the dead volume. Appropriate corrections for the pressure drop along the column were made on the basis of the pressure at the injection and outlet ports. The retention times and peak areas were based on the average of several injections for each sample and condition. Adsorbate amounts from 0.1 to 10 μl were injected.

The following compounds, supplied from various commercial sources, were used as IGC adsorbates: *n*-hexane (*n*-C₆H₁₄), benzene, chloroform (CHCl₃), and tetrahydrofuran (THF), as representatives of aliphatic, aromatic, acid, and basic compounds, respectively. They were of HPLC grade and used as received.

RESULTS AND DISCUSSION

The fronts of all peaks were vertical and sharp suggesting that the predominant factor governing the bandwidth was isotherm curvature, typical for finite coverage conditions IGC (Fig. 1). However, with very small injection volumes ($\ll 0.1 \mu\text{l}$), the peaks tended to become Gaussian. The points of each peak maximum for different injected amounts of the adsorbate resulted in a characteristic line, drawn when the peaks were superimposed.⁴

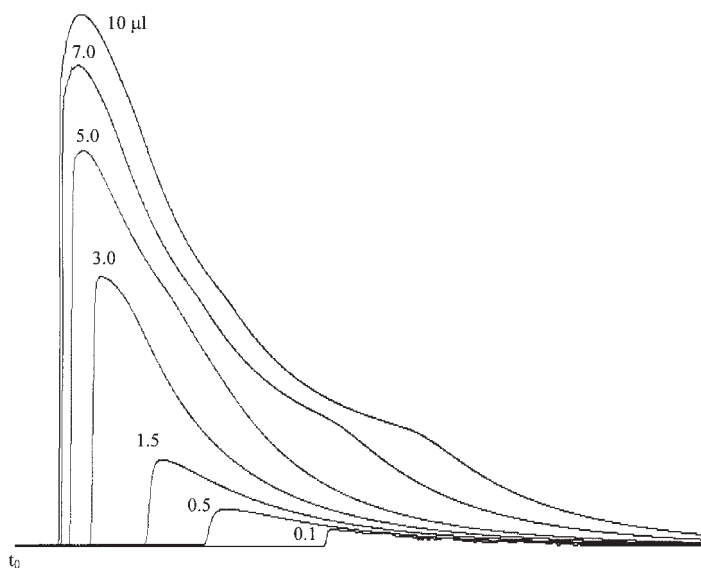


Fig. 1. Chromatographic peaks obtained for different amounts of benzene (0.1, 0.5, 1.5, 3.0, 5.0, 7.0, 10 μl) on solid II. $T = 423 \text{ K}$.

Monolayer coverage and specific surface area

The adsorption isotherms for the selected compounds (*n*-C₆H₁₄, CHCl₃, benzene, and THF) on solids I, II, and III were obtained in the range 383–423 K. The adsorption isotherms of *n*-C₆H₁₄ for all three sorbents are presented in Fig. 2 for two temperatures. The isotherms of the selected organics on solid I are shown in Fig. 3. For the

sake of clarity only some of the plots are displayed in Figs. 2 and 3, but similar curve shapes were observed for the adsorption of other probes.

The $\alpha = f(p)$ plots were converted to the linear form of the well-known BET isotherm^{7,8}:

$$\frac{p/p_0}{\alpha(1-p/p_0)} = \frac{1}{\alpha_m C} + \frac{(C-1)}{\alpha_m C} (p/p_0) \quad (4)$$

where C is a constant related to the heat of adsorption, and α_m is the amount of adsorbate adsorbed in a monolayer. The p_0 values were calculated according to the Antoine equation using literature data for n -C₆H₁₄,⁹ CHCl₃,¹⁰ benzene¹⁰ and THF.¹¹ In the linear range of the adsorption isotherms ($0.05 \leq p/p_0 \leq 0.3$), α_m and C were estimated from the slope and the intercept of the straight line according to Eq. (4). The BET plots in the indicated range gave excellent linearity for each adsorbate ($r \geq 0.999$), except for CHCl₃ on substrate I where the correlation coefficients were slightly lower ($r \geq 0.991$). The obtained data for C , and α_m , are collected in Table I.

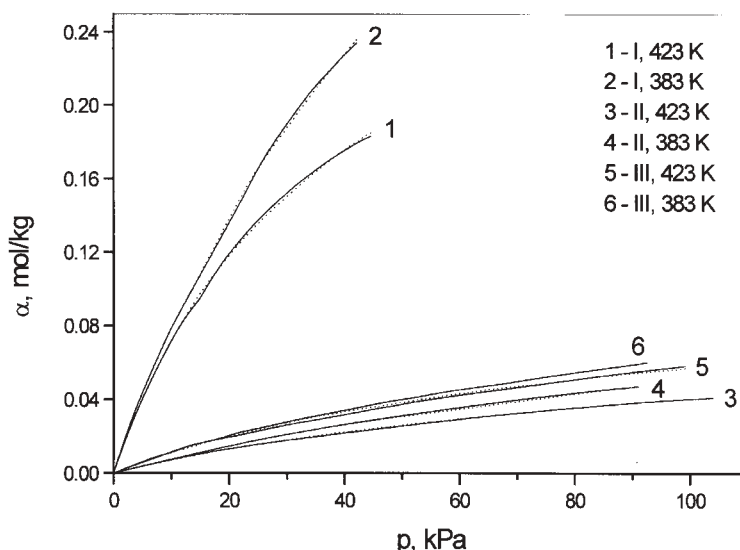


Fig. 2. Adsorption isotherms of n -hexane on solids I, II, and III, at 423 and 383 K (dotted lines represent BET fits).

The adsorption of n -hexane occurs *via* dispersive forces. The other three adsorbates have the ability to establish specific interactions with the chromia surfaces. Previous IGC measurements at zero surface coverage² showed the highly basic character of solid I, the basic character of II, and the slightly basic character-close to amphoteric character of solid III. Therefore, THF is expected to establish repulsive forces with the surface hydroxyl groups, whereas CHCl₃ acts as a strong Lewis acid. It could be expected that the difference in the acid-base interactions of these two compounds with the surfaces become insignificant when multilayer coverage exists.

The specific surface area of the solids, S_a , may be estimated from the adsorption isotherm of the selected adsorbate using the following relation:

$$S_a = \alpha_m \sigma N \quad (5)$$

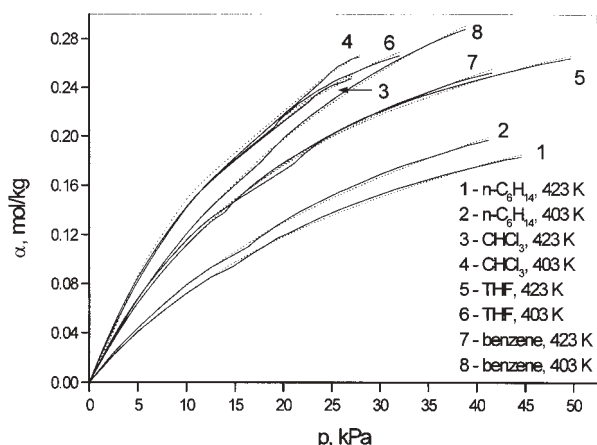


Fig. 3. Adsorption isotherms of the selected organics on solid I, at 423 and 403 K (dotted lines represent BET fits).

For the calculation of the area of a solid covered by an adsorbate molecule, σ , it was presumed that each adsorbate molecule had twelve nearest neighbors in a close hexagonal packing, arranged on the solid surface in the same way as on a plane surface immersed into the bulk liquid of the adsorbate.¹² This approach is common in IGC.¹³⁻¹⁵ Accordingly, the molecule area of contact with the chromia is:

$$\sigma = A_s \left(\frac{M}{N\rho} \right)^{2/3} \quad (6)$$

where M , N , and ρ are readily available, and $A_s = 1.091$. The factor A_s clearly depends on the way the molecules are packed on the surface with monolayer coverage. This varies for a given adsorbate depending on the nature of the solid, and the mobility of the adsorbed molecules. Except for spherically symmetrical molecules, the factor A_s is also influenced by the orientation of the molecules relative to the surface. In this work the effective dimensions of the adsorbate molecules and the way they are packed together in the films were not evaluated. Instead, the numerical values of S_a of the selected organic molecules obtained from Eq. (5) were compared with the BET specific surface areas of solids measured by the nitrogen gas adsorption method.

The specific surface areas of the three chromias are shown in Table II, from which it is evident that chromia I has the highest S_a value, chromia II the lowest, while chromia III has a slightly higher value than chromia II. However, the S_a values are temperature dependent, which results from the density gradient across the temperature range.

Comparing the specific surface areas obtained by IGC and by the standard N_2 gas adsorption method, it can be seen that the data for samples I and II agree reasonably

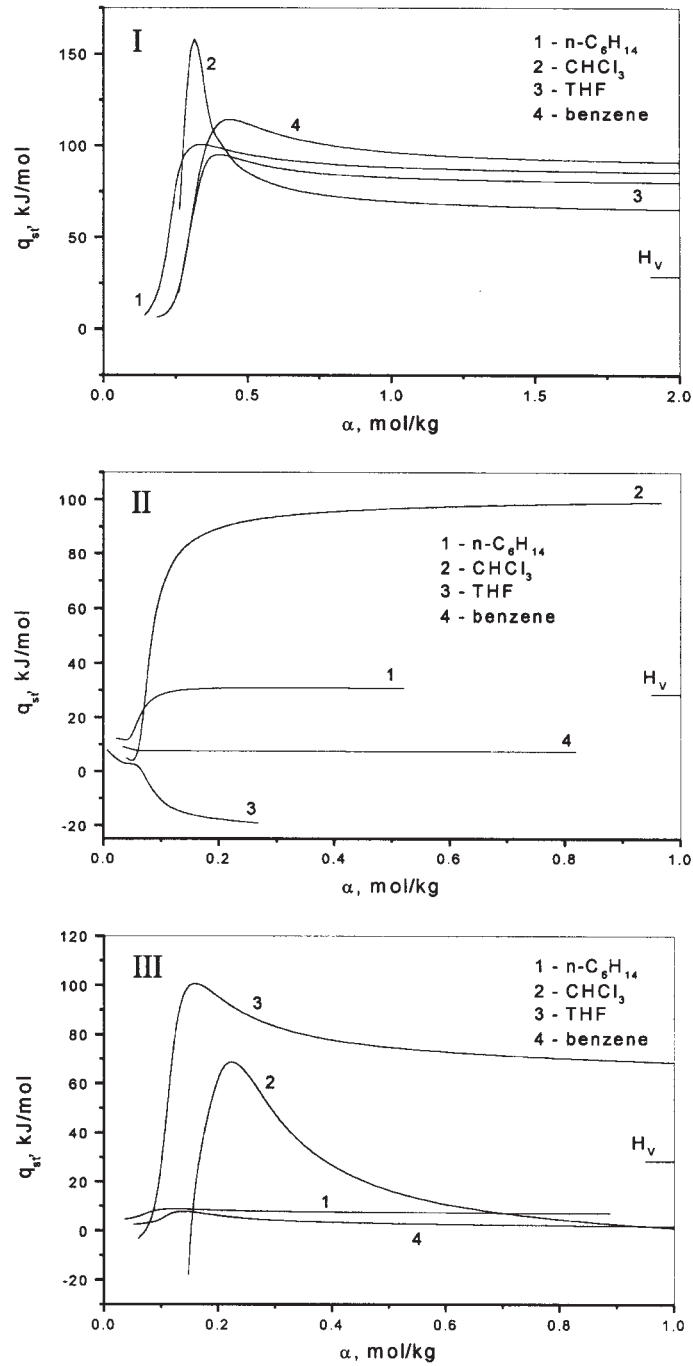


Fig. 4. Isosteric heat of adsorption for $n\text{-C}_6\text{H}_{14}$, CHCl_3 , THF, and benzene, as a function of surface coverage (solids: I, II, III).

well, S_{a/N_2} (I) = 75 m²/g, and S_{a/N_2} (II) = 9 m²/g. However, in the case of sample III, the BET result is much lower S_{a/N_2} (III) = 4 m²/g. Repeated measurements, using both techniques, confirmed the values obtained. Further evaluation is needed to elucidate discrepancy in S_a and S_{a/N_2} . One thought is that the IGC adsorbate has a greater ability to associate with the chromia surface. The mechanism can be explained by the fact that there is a great number of hydroxyl groups interacting through donor-acceptor type interactions, as well as through dispersive forces. Hence, the thermally treated solid II has a more homogeneous surface, and lower number of active hydroxyl groups capable of interacting with adsorbate molecules, and as a consequence, surface I is much larger.

TABLE I. BET equation constant C , and monolayer capacity, a_m , for chromias (I, II, and III) in the temperature range 383 – 423 K

Adsorbate	T/K	C			$a_m/\text{mol kg}^{-1}$		
		I	II	III	I	II	III
$n\text{-C}_6\text{H}_{14}$	423	26.2	8.09	8.60	0.280	0.061	0.090
	413	19.1	7.65	9.04	0.301	0.055	0.083
	403	14.6	7.50	8.20	0.318	0.052	0.074
	393	12.2	8.07	9.47	0.321	0.044	0.065
	383	8.44	7.91	7.13	0.362	0.045	0.060
CHCl_3	423	50.9	5.67	13.9	0.406	0.081	0.173
	413	37.4	6.49	14.1	0.419	0.075	0.154
	403	27.7	9.25	12.3	0.456	0.074	0.131
	393	16.8	9.29	11.3	0.480	0.064	0.112
	383	13.2	9.32	12.1	0.539	0.056	0.102
THF	423	40.9	7.41	20.5	0.348	0.067	0.120
	413	34.3	6.47	14.3	0.362	0.068	0.114
	403	31.4	6.26	18.1	0.386	0.060	0.098
	393	21.1	7.62	13.6	0.422	0.055	0.073
	383	13.9	7.91	13.9	0.492	0.051	0.065
benzene	423	31.3	7.50	14.1	0.371	0.068	0.105
	413	24.3	7.29	13.2	0.402	0.064	0.093
	403	17.2	7.56	12.0	0.452	0.059	0.082
	393	12.0	7.51	11.6	0.477	0.056	0.069
	383	9.85	7.44	11.8	0.498	0.051	0.057

TABLE II. Specific surface areas, S_a , of chromias (I, II, and III) in the temperature range 383–423 K

Adsorbate	T/K	$S_a / \text{m}^2 \text{g}^{-1}$		
		I	II	III
$n\text{-C}_6\text{H}_{14}$	423	66.7	14.5	21.5
	413	71.8	14.4	19.7
	403	75.7	13.1	17.7
	393	76.5	12.3	15.5
	383	86.2	10.5	14.9
CHCl_3	423	69.2	13.7	29.5
	413	71.3	12.7	26.2
	403	77.7	12.5	22.4
	393	83.2	10.9	19.0
	383	91.9	9.55	18.1
THF	423	60.2	11.6	20.8
	413	62.7	11.7	19.6
	403	66.8	10.4	16.9
	393	72.1	9.54	12.6
	383	85.0	8.83	11.3
benzene	423	68.0	12.5	19.2
	413	69.8	11.7	17.0
	403	72.7	10.9	15.0
	393	75.4	10.3	12.6
	383	82.8	9.42	11.2

Isosteric heat of adsorption

The isosteric (at constant surface coverage) heat of adsorption, q_{st} , is determined using the Clausius-Clapeyron equation, as follows:

$$\left[\frac{\partial(\ln p)}{\partial(1/T)} \right]_{\alpha} = -\frac{q_{st}}{R} \quad (7)$$

Fig. 4 presents plots of q_{st} versus α for the indicated adsorbate. It is clear from Fig. 4 that the variation of q_{st} with α is very complex. Distinct maxima for q_{st} are observed for all adsorbates on solids I and III. These extremes correspond to the maxima of adsorption energy, and are located in the vicinity of the corresponding monolayer surface capacity. With low coverage, very great changes in the q_{st} values are noted, depending on the adsorbate. With increasing adsorbed amount, q_{st} approaches a constant value. This indicates strong adsorbate/surface interactions at the beginning of the adsorption process, but not in all instances, *i.e.*, for all adsorbates, the attractive forces are predominant. It is common in IGC that the q_{st} values at higher surface load-

ing approach asymptotically the respective heats of evaporation, $\Delta_{\text{vap}}H$.^{14–18} This results from the conversion of the adsorption-desorption process into evaporation from the pure liquid surface. However, as reported, in some cases q_{st} may follow an unexpected trend, particularly at low coverage.¹⁸ In the present work, the difference between q_{st} and $\Delta_{\text{vap}}H^0$ in most adsorbate/adsorbent combinations suggests a strong influence of the solid surface on the adsorbate uptake even beyond a monolayer. The isosteric heats of adsorption of $n\text{-C}_6\text{H}_{14}$, and CHCl_3 on the solid II surface showed no maximum. They asymptotically approached a constant value, which was below the bulk heat of evaporation $\Delta_{\text{vap}}H^0$, for THF and benzene, equal to $\Delta_{\text{vap}}H^0$ for $n\text{-C}_6\text{H}_{14}$, but greatly exceeding $\Delta_{\text{vap}}H^0$ for CHCl_3 .

Adsorption energy distribution

For the quantitative interpretation of the surface energetic heterogeneity, the adsorption energy distribution function, χ , related to the isotherm $\alpha(p, T)$ can be found from the equation:

$$\alpha(p, T) = \text{am} \int_0^{\infty} \chi(\varepsilon) \theta(\varepsilon, p, T) d\varepsilon \quad (8)$$

where $\theta(\varepsilon, p, T)$ is the local isotherm of surface sites with the same ε . To calculate χ , the terms derived by Rudzinski *et al.*¹⁹ were used:

$$\chi = -\frac{\partial \alpha}{\partial \varepsilon} + \frac{3.14^2}{6} R^2 T^2 \frac{\partial^3 \alpha}{\partial \varepsilon^3} \quad (9)$$

where the ε function was estimated as:

$$\varepsilon = -RT \ln \frac{p}{K_p} - zu \frac{\alpha}{\alpha_m} \quad (10)$$

using $zu = \Delta_{\text{vap}}H^0/4$,²⁰ and $K_p = p_0 \exp(\Delta_{\text{vap}}H^0/RT)$.²¹ The values for $\Delta_{\text{vap}}H^0$ were taken from the literature.²² From the obtained isotherms, the functional dependencies of p on α were derived, and the latter was applied to calculate ε and χ .

The adsorption energy distribution functions of the adsorption sites measured with benzene on solid II are shown in Fig. 5 for three temperatures. The distribution functions for the selected adsorbates on solid II are presented in Fig. 6. Distribution functions on solids I, II, and III, measured with benzene at 423 K, are given in Fig. 7.

The obtained dependencies relating the number of sites with a given energy to discrete adsorption energy values vary from one solid/adsorbate pair to another in terms of the site number, but do not vary significantly in terms of the curve shapes. Both the shifting of peaks toward higher energies, and a much larger number of sites at higher temperature were observed. The values of χ when CHCl_3 was the adsorbate are several times higher than those of the other adsorbates, which is attributed to the strong acid-base forces. Generally, χ is not only a characteristic of the solid itself, but is strongly dependent on the type of the solid/adsorbate combination as well.²³ As a consequence of the more intensive adsorption on solid I, the χ values are uniformly

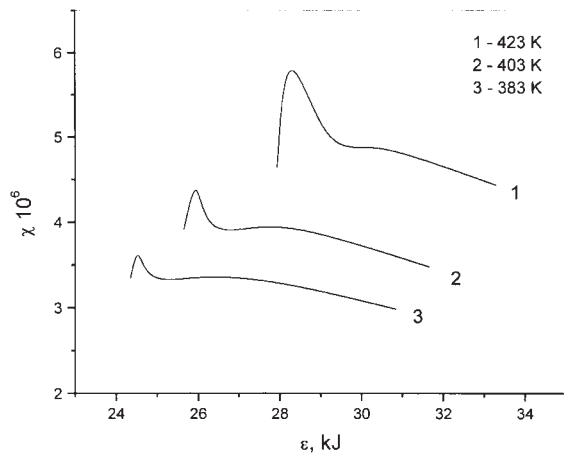


Fig. 5. Distribution function of the adsorption sites on solid II, at different temperatures, measured with benzene.

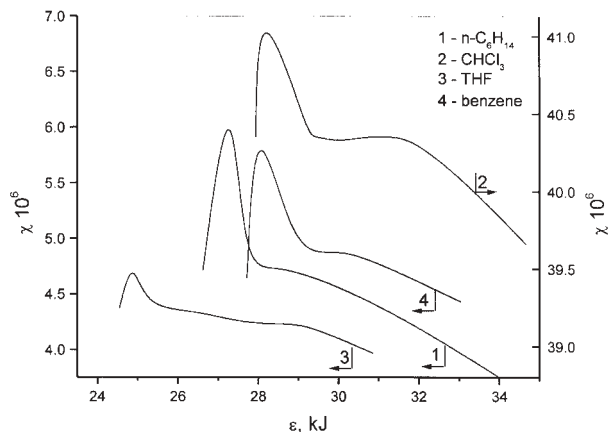


Fig. 6. Distribution function of the adsorption sites on solid II, measured with the selected adsorbates at 423 K.

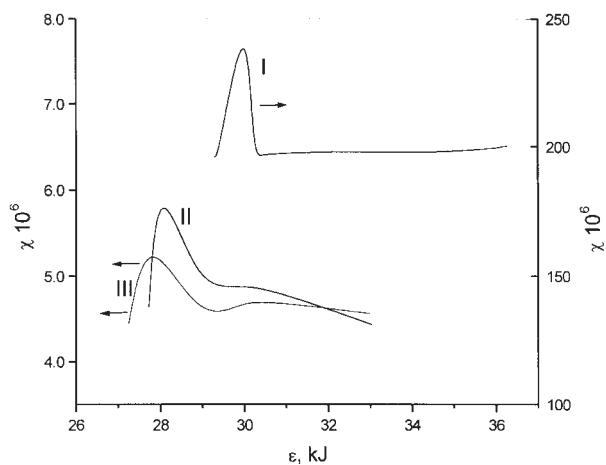


Fig. 7. Distribution function of the adsorption sites on solid I, II, and III, measured with benzene at 423 K.

higher, which suggests that thermal treatment causes a reduction in the number of sites on the chromia surface.

Spreading pressure

The spreading pressure, π , is defined as the difference between surface free energy at the solid/gas interface and the solid/liquid interface.²⁴ It is dependent on the uptake of adsorbate vapour onto the solid surface. To estimate π the integrated form of Gibbs' adsorption equation¹³ was used:

$$\pi = \frac{RT}{S_p M} \int_0^{p/p_0} \frac{\alpha}{p/p_0} d(p/p_0) \quad (11)$$

Typical plots of π versus p/p_0 , for $n\text{-C}_6\text{H}_{14}$ at five different temperatures are given in Fig. 8. The spreading pressures at saturated vapour, π^0 ($p/p_0 = 1$, $\pi = \pi^0$), were estimated by extrapolating the function $\pi = f(p/p_0)$ to $p/p_0 = 1$. The values of π^0 are presented in Table III.

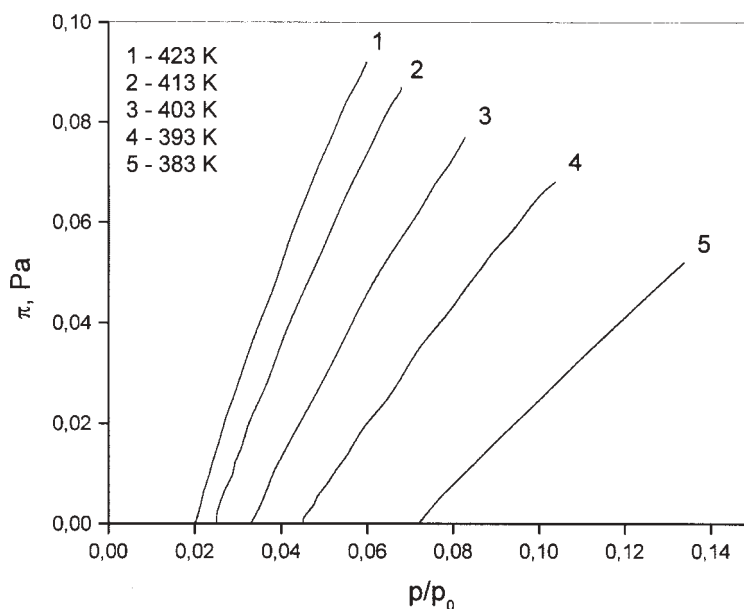


Fig. 8. Spreading pressures of n -hexane on solid II, at different temperatures.

TABLE III. Spreading pressures, π^0 , of the selected adsorbates at $p = p_0$

Adsorbate	T/K	π^0/Pa		
		I	II	III
$n\text{-C}_6\text{H}_{14}$	423	49.4	2.01	1.87
	413	18.0	1.72	1.32
	403	9.11	1.10	1.03
	393	4.97	1.05	0.99
	383	1.88	0.72	0.97

TABLE III. (Continued)

Adsorbate	T/K	π^0/Pa		
		I	II	III
CHCl_3	423	451	4.90	2.17
	413	198	3.39	1.44
	403	80.8	2.01	1.17
	393	30.8	1.70	1.00
	383	9.06	1.58	0.97
THF	423	127	19.1	0.80
	413	105	13.4	0.50
	403	101	7.59	0.48
	393	20.1	2.22	0.44
	383	2.25	2.45	0.37
benzene	423	95.3	8.66	1.44
	413	41.2	7.65	1.19
	403	20.5	3.56	1.06
	393	8.32	3.22	0.92
	383	3.62	2.11	0.91

The parameter π , as a measure of the decrease in the surface energy due to adsorption, becomes higher with increasing coverage. Also, the π values are uniformly higher at higher temperatures. Commonly, for lower π values, lateral adsorbate/adsorbate interactions are negligible, but the adsorbate/adsorbent forces are strong. On the other hand the reverse occurs at higher π values.

CONCLUSIONS

The adsorption of *n*-hexane, chloroform, benzene, and tetrahydrofuran on two types of solids obtained from a colloidal chromia dispersion and a commercial chromia were analyzed using the BET theoretical model. The properties of the solid surface as well as the nature of the adsorbate govern the uptake of adsorbate by chromia. The isosteric heat of adsorption approaches the constant value with increasing adsorbate loading. The adsorption energy distribution values differ for each solid/adsorbate pair, in terms of the site number, but show similar trends. The estimated spreading pressures, at saturated vapour, decrease gradually with temperature. Chloroform, due to its ability to establish strong acid-base interactions, exhibits very intensive adsorption. Comparing the adsorption data obtained for dried and heated chromia, it can be concluded that the applied heat treatment leads to a reduction in the number of active adsorption sites and, therefore, produces more homogeneous surfaces.

LIST OF SYMBOLS

- I, II – solids from colloidal chromia
 III – commercial chromia
 A_S – packing factor (for S_a correction)
 F_c – corrected carrier gas flow rate ($\text{m}^3 \text{s}^{-1}$)
 h – height of the chromatographic peak (V)
 j – James-Martin gas compressibility correction factor
 m – mass of sorbent in the column (kg)
 α – adsorbed amount per mass of adsorbent (mol kg^{-1})
 N – Avogadro's number, ($6.023 \times 10^{23} \text{ mol}^{-1}$)
 n – injected amount of adsorbate (mol)
 p – partial vapour pressure of adsorbate (Pa)
 p_0 – saturated vapour pressure of adsorbate (Pa)
 S – area of the chromatographic peak (bounded by envelope) (s V)
 S_a – specific surface area of sorbent obtained by IGC ($\text{m}^2 \text{g}^{-1}$)
 S_{a,N_2} – specific surface area of sorbent obtained by BET with N_2 adsorption ($\text{m}^2 \text{kg}^{-1}$)
 S_{ads} – area that is bounded by the vertical line drawn from t_0 to t_R including the rest of S (s V)
 R – gas constant ($8.31441 \text{ J mol}^{-1} \text{ K}^{-1}$)
 r – correlation coefficient for linear regression
 T – column temperature (K)
 t_0 – retention time of an unretained compound (methane)(s)
 t_R – adsorbate retention time (s)
 V_N – adsorbate net retention volume (m^3)
 C – BET constant
 a_m – monolayer capacity of the adsorbent (mol kg^{-1})
 ϵ – condensation energy (J)
 θ – local isotherm on sites with the same ϵ
 σ – adsorbate molecule area (m^2)
 θ_{st} – isosteric heat of adsorption (J mol^{-1})
 $\Delta_{\text{vap}}H^\circ$ – heat of evaporation (J mol^{-1})
 M – molar mass of adsorbate (kg mol^{-1})
 π – spreading pressure of adsorbate at p (Pa)
 π_0 – spreading pressure of adsorbate at $p = p_0$ (Pa)
 ρ – density (kg m^{-3})
 χ – adsorption energy distribution function

ИЗВОД

ИНВЕРЗНА ГАСНА ХРОМАТОГРАФИЈА НА ХРОМ(III)-ОКСИДУ. ДЕО II.

А. Е. ОЊИА*, С. К. МИЛОЊИЋ* и Љ. В. РАЈАКОВИЋ**

*Институт за нуклеарне науке "Винча", б. бр. 522, 11001 Београд и **Технолошко-металуршки факултет,
б. бр. 494, 11001 Београд

Испитиване су интеракције *n*-хексана, хлороформа, тетраhydroфурана и бензена, са површинама чврсте фазе лабораторијски добијеног колоидног хром(III)-оксида и комерцијалног хром(III)-оксида, методом инверзне гасне хроматографије (IGC) при коначној прекривености. Адсорпционе изотерме су добијене за два узорка чврсте фазе добијене из сола хром(III)-оксида, сушену чврсту фазу сола (423 К, узорак I), аморфне, и жарену (1073 К, узорак II), кристалне структуре, као и за комерцијални хром(III)-оксид кристалне структуре, у температурном опсегу 383 – 423 К. Из добијених изотерми израчунате су: вредности специфичних површина, функције расподеле енергије на површини, изостеричне топлоте адсорпције и притисак адсорбата на површинама. Значајно мања адсорпциона моћ узорка II приписана је дехидроксилацији површине у току претходног третмана на високим температурама. У оба случаја чврста површина показује појачани афинитет према хлороформу, услед успостављања снажних кисело-базних интеракција.

(Примљено 5. јула 2001)

REFERENCES

1. V. Henrich, P. Cox, *Surface Science of Metal Oxides*, Cambridge Univ. Press, 1994
2. A. Onjia, S. Milonjić, Lj. Rajaković, *J. Serb. Chem. Soc.* **66** (2001) 259
3. R. J. Laub, R. L. Pecsok, *Physicochemical Applications of Gas Chromatography*; Wiley-Interscience, New York, 1978
4. J. R. Conder, C. L. Young, *Physicochemical Measurement by Gas Chromatography*; Wiley-Interscience, New York, 1979
5. A. T. James, A. J. P. Martin, *Biochem J.* **50** (1952) 679
6. A. Kiselev, Ya. Yashin, *Gas-Adsorption Chromatography*, Plenum Press, New York, 1969
7. S. Brunauer, P. H. Emmett, E. Teller, *J. Am. Chem. Soc.* **60** (1938) 309
8. S. Brunauer, S. Deming, L. Deming, P. Emmett, *J. Am. Chem. Soc.* **62** (1940) 1723
9. C. B. Williamham, W. J. Taylor, J. M. Pignocco, F. D. Rossini, *J. Res. Natl. Bur. Stand. (USA)* **35** (1945) 219
10. D. R. Stull, *Ind. Eng. Chem.* **39** (1947) 517
11. D. W. Scott, *J. Chem. Thermodyn.* **2** (1970) 833
12. P. H. Emmett, S. Brunauer, *J. Am. Chem. Soc.* **59** (1937) 1553
13. G. Dorris, D. Gray, *J. Colloid Interface Sci.* **71** (1979) 93
14. M. Kopečni, J. Čomor, M. Todorović, Lj. Vujisić, D. Vučković, *J. Colloid Interface Sci.* **134** (1990) 376
15. S. Katz, D. Gray, *J. Colloid Interface Sci.* **82** (1981) 326
16. M. Kopečni, S. Milonjić, W. Rudzinski, J. Jagiello, *Collect. Czech. Chem. Commun.* **52** (1986) 572
17. E. Papirer, S. Li, H. Balard, J. Jagiello, *Carbon* **29** (1991) 1135
18. N. Djordjević, R. Laub, M. Kopečni, S. Milonjić, *Anal. Chem.* **58** (1986) 1395
19. W. Rudzinski, J. Jagiello, Y. Grillet, *J. Colloid Interface Sci.* **87** (1982) 478
20. W. A. House, M. J. Jaycook, *J. Colloid Polym. Sci.* **256** (1978) 52
21. M. Jaroniec, *Surf. Sci.* **50** (1975) 553
22. V. Majer, V. Svoboda, *Enthalpies of Vaporization of Organic Compounds: A Critical Review and Data Compilation*, Blackwell Scientific Publications, Oxford, 1985, p. 300
23. D. H. Everett, *Langmuir* **9** (1993) 2586
24. J. H. de Boer, *The Dynamical Character of Adsorption*, Oxford Univ. Press, 2nd ed. 1968.